

# The Influence of Solvent Type and Polymer Concentration on the Physical Properties of Solid State Polymerized PA66 Nanofiber Yarn

Razieh Hashemi Sanatgar,<sup>1</sup> Sedigheh Borhani,<sup>1</sup> Seyed Abdolkarim Hosseini Ravandi,<sup>1</sup> Ali Akbar Gharehaghaji<sup>2</sup>

<sup>1</sup>Department of Textile Engineering, Nanotechnology and Advanced Materials Institute, Isfahan University of Technology, 84156 83111 Isfahan, Iran

<sup>2</sup>Department of Textile Engineering, Amirkabir University of Technology, Tehran, Iran

Received 16 August 2011; accepted 20 January 2012

DOI 10.1002/app.36871

Published online in Wiley Online Library (wileyonlinelibrary.com).

**ABSTRACT:** We investigated the effects of two different solvent types and three solution concentrations on the electrospinning of solid state polymerized polyamide 66 (SSP PA66) nanofiber yarns. Nanofiber yarns were electrospun from SSP PA66 solutions in formic acid and formic acid/chloroform (3/1), using two oppositely metallic spinnerets system. Scanning electron microscopy (SEM) and X-ray diffraction (XRD) were employed to characterize the morphology and properties of the nanofibrous yarns. Experimental results show that adding chloroform to formic acid as a binary solvent increases viscosity of polymer solution and the nanofibers diameter significantly. XRD patterns reveal that the presence of chloroform affects the

crystallinity and the mechanical properties of the produced nanofibrous yarns. PA66 nanofiber yarn from 10 wt % formic acid/chloroform (3/1) solution was successfully electrospun with strength and modulus of 120.16 MPa and 1216.27 MPa respectively. It is also shown that the solution concentration has a significant effect on the modulus of the nanofibers yarns. © 2012 Wiley Periodicals, Inc. *J Appl Polym Sci* 000: 000–000, 2012

**Key words:** nanotechnology; nanofibers yarn; solid state polymerized polyamides; mechanical properties; X-ray diffractometry; scanning electron microscopy; solvent type; solution concentration

## INTRODUCTION

Recently, electrospinning has attracted huge attention as a technique that is very simple and inexpensive to manufacture submicron fibers and nanofibers.<sup>1</sup> Customary electrospinning equipment consists of four main parts: a metallic spinneret, a high voltage source, a pump and a collector. During the electrospinning process, an electrical potential is being applied to a polymer droplet flowing out from the tip of a needle. Charging the droplet results in the formation of a flow phenomenon known as Taylor Cone. When the electrical forces overcome the surface tension of polymer solution, a charged fluid jet is ejected following a spiral path.<sup>2</sup> The electrical forces elongate the jet thousands of times and the jet stretches toward the grounded electrode. Electrospun nanofibers are often collected as randomly oriented structures in the form of nonwoven mats which have already had interesting applications in fields of filtration, protective clothing, self-cleaning,

drug delivery, tissue engineering, electronic and photonic devices, etc.<sup>3–9</sup>

For some polymers, the strength of a single nanofiber may be so weak for conventional physical manipulation due to its small size and low mechanical strength and as a result, it breaks under its own weight.<sup>10</sup> Meanwhile, obtaining continuous aligned nanofibers and high-volume production is very important for many areas such as fiber reinforcement and device manufacture.<sup>11</sup>

Various structures such as aligned nanofibers, arrayed nanofibers, and uniaxially aligned electrospun nanofibers yarn have been achieved using different mechanical collection devices and manipulating the electric field.<sup>12</sup> Aligned nanofibers in particular can be tailored for use in microelectronics, photonics and in a variety of electrical, optical, mechanical, and biomedical applications.<sup>13</sup>

Up to the end use, a new generation of yarns can be engineered to be used in new fields such as tissue scaffolds and reinforcement materials in composites<sup>14</sup> which have functions different from nanowebs. Collecting nanofibers in arrays and inserting twist in this bundle initiates a new nanofibrous material as nanofiber yarn. Continuous nanoyarns were produced by modifying the electric field in a limited linear density.<sup>15,16</sup> Some of these techniques

Correspondence to: S. Borhani (sborhani@cc.iut.ac.ir).

**TABLE I**  
**Solvent Characterization**

Solvent	Electrical conductivity, $K$ ( $\mu\text{S}/\text{cm}$ ) 25°C	Surface tension, $\tau$ (mN/m) 20°C	Zero shear viscosity, $\eta_0$ (cP)
Chloroform	0.13	27.16	0.58
Chloroform/acid formic (1 : 3)	359	30.24	1.32
Acid formic (98–100%)	884	38.36	1.57

have used a liquid media in a static<sup>17,18</sup> or dynamic state,<sup>19</sup> to produce continuous yarn. The two oppositely metallic spinnerets are a system for producing uniaxially aligned electrospun nanofibers yarn.<sup>20</sup>

There are many parameters which can influence the transformation of polymer solutions into nanofibers through electrospinning. These parameters include: (1) the solution properties such as viscosity, elasticity, conductivity, and surface tension, (2) controlled variables such as hydrostatic pressure in the spinneret, electric potential at the tip, and the distance between the tip and the collection screen, and (3) ambient parameters such as temperature, humidity, and air velocity in the electrospinning chamber.<sup>21,22</sup>

The electrospinning of PA66 has been done by other researchers<sup>23–29</sup>: Huber et al.<sup>27</sup> described the use of electrospun PA66 microfilaments as part of a parallel aligned polymer microfiber array to guide the spatial reconstruction of murine C2C12 myotubes *in vitro* without the use of additional surface modifications or a feeder layer.

Lingaiah et al.<sup>28</sup> studied the influence of collector drum speeds, electrospinning setups (single and multiple-spinneret) and polymer concentrations on the morphology, uniformity, and mechanical properties of the PA66 polymer nanofiber fabrics. Guerrinia et al.<sup>16</sup> analyzed the influence of the PA66 molecular weight and terminal carboxylic and amines groups on the electrospinning.

Although some researches have been done on the electrospinning of PA66 nanofiber mats, there is no report on PA66 nanofiber yarns and their properties. Therefore, in this work, the influence of the polymer concentration and solvent type were investigated using two oppositely metallic spinnerets system. Solid state polymerized PA66 nanofiber yarns were produced with improved mechanical properties from low concentration polymer solution using formic acid and chloroform combination as the solvent.

## EXPERIMENTAL

### Materials

Solid state polymerized PA66 (SSP PA66) with 77,874 g/mol molecular weight ( $M_w$ ) was obtained

from Zanjan Tire Cord company. Solid state polymerization was done in 4360 (kg/h) N<sub>2</sub> flow at 168.5°C, during 15.1 h.

Two different solvents were used for the electrospinning solutions: (a) formic acid (98–100%, from Merck) with density of 1.22 g/mL at 20°C and boiling point of 101°C and (b) mixture of formic acid and chloroform with the ratio of 3 : 1 in which chloroform with the density of 1.47 g/mL at 20°C and boiling point of 61°C was obtained from Merck.

### Solutions preparation and characterization

Polymer solutions were prepared by the dissolution of SSP PA66 in formic acid and mixture of formic acid and chloroform (3 : 1). The solvents electrical conductivities were measured in a conduct meter from Jenway, model 3540. The surface tension of solvents was measured using a tension meter from Data Physic; model DCAT2 at 20°C. The shear viscosity of the solutions at low shear rates was measured in a rotating rheometer, from Brookfield, model DV-II+Pro. Solvents characterization is shown in Table I.

### Electrospinning setup

The process of electrospun nanofiber yarn production is as follows: Two charged metallic spinnerets were placed opposite to each other (part C in Fig. 1). A neutral plate was placed in the middle of the electric field (part B in Fig. 1). Electrostatic induction happened in the neutral plate: it means that

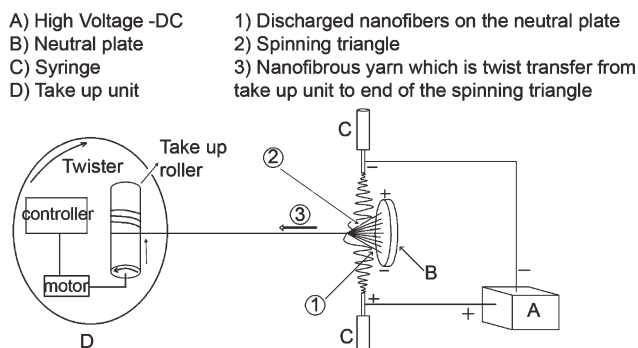


**Figure 1** Schematic of the mechanism of yarn formation.

TABLE II  
Electrospinning Conditions of Samples

Sample	Solution concentration (wt %)	Applied voltage (kV)	Feeding rate (mL/h)	Twist (TPM)	Take up speed (cm/h)	Distance between two needles (cm)	Distance between needles center and neutral surface (cm)	Distance between needles center and collector (cm)
SSP-cl	10	12	0.244					
SSP-cl	18	10	0.244					
SSP	10	12	0.244	4470	152	18	3	22
SSP	14	12	0.293					
SSP	18	10	0.244					

SSP, solid state polymerized PA66/acid formic; SSP-cl, solid state polymerized PA66/acid formic + chloroform.

electrons on the surface of the plate were displaced in such a way that half of them became positively charged and the others negatively charged. Two charged jets of polymer solution were pulled out of spinnerets and attracted toward the side of the inductive plate with opposite charge (part B in Fig. 1) making the jets neutralized. Electrospun nanofibers were collected onto the plate (part 1 in Fig. 1).

Electrospun nanofibers came into contact with a piece of yarn used as a linkage and placed in their path; then, the other end of the nanofiber was pulled toward the plate, making a spinning triangle (part 2 in Fig. 1). The nanofibers were then twisted by rotating piece yarn around its axis. A take-up unit was used which was able to twist and take up yarn without any balloon formation (part D in Fig. 1). The solutions electrospinning was done at room temperature (25°C) and without room humidity control.

Table II shows the electrospinning conditions in which each sample was processed.

### Structural and morphological characterization

#### Scanning electron microscopy

After gold coating, a scanning electron microscope (Philips SEM XL-30) was used to characterize the morphology of the electrospun nanofiber yarns. High magnification SEM images were taken to measure the diameter of nanofibers. The diameters of 100 nanofibers were measured by means of Measurement Software and compared with the image scale. Finally, the average of the results was obtained.

#### Mechanical characterization

Before the experiment, yarns were in standard conditions (20 ± 2°C and 65% RH) for 24 h. The mechanical properties of yarn were measured by Zwick 1446-60. Zwick was designed for constant rate of elongation. To obtain stress-strain curves, the sample length was 2.5 cm with cross head speed of 60 mm/min.

#### X-ray diffractometry

Wide angle X-ray diffraction (WAXD) patterns of the PA66 nanofibrous yarns were recorded by a Philips X-ray diffractometer using Ni-filtered Cu K $\alpha$  (wavelength,  $\lambda = 1.54 \text{ \AA}$ ) radiation. The diffraction scans were collected at  $2\theta = 5\text{--}50^\circ$ . The scan speed was  $0.04^\circ/\text{s}$ . The area under the crystalline and amorphous portions was determined in arbitrary units using the Origin software and the degree of crystallinity (%) was calculated using the following equation:

$$X(\%) = \frac{A_c}{A_c + A_a} \times 100$$

where  $A_c$  and  $A_a$  are the integrated intensity corresponding to the crystalline and amorphous phases, respectively.

## RESULTS AND DISCUSSION

### Solvent type

Generally, formic acid is used as a solvent for the dissolution of PA66. However, its boiling point of 100°C is relatively high and therefore, it is not very suitable for electrospinning. Nevertheless, the boiling point of formic acid can be lowered by addition of a cosolvent with a relatively low boiling point (bp), namely chloroform (bp of 61°C).<sup>25</sup> Gogolewski and Pennings<sup>30</sup> found that the ratio of formic acid to chloroform of 75/25 (v/v) gave the highest tensile strength fiber when a high molecular nylon 6 was used for making dry spun fibers. A low volatility solvent is required for dry spinning and electrospinning processes. If solvent is not evaporated completely during the electrospinning process, it is very difficult to form a nanofiber yarn or remove the electrospun yarn from the take up drum.

So the highest (18 wt %) and lowest (10 wt %) solution concentration of SSP PA66, which was capable of producing nanofibrous yarn in two solvent systems, was determined. Table III shows the zero

**TABLE III**  
Zero Shear Viscosity,  $\eta_0$ , and the Nanofiber Diameter

Sample	Solution concentration, C (wt %)	Zero shear viscosity, $\eta_0$ (cP)	Fiber diameter	
			Number-average (nm)	CV %
SSP	18	2479	246	25.9
SSP-cl	18	6099	1080	20.9
SSP	10	324	117	16.03
SSP-cl	10	452	199	12.76

shear viscosity,  $\eta_0$ , and the nanofiber diameter of each sample.

The results show that adding chloroform to acid formic as a binary solvent increases viscosity of polymer solution at the same concentration. The increase in viscosity for 18 and 10 wt % concentrations was 145 and 40%, respectively.

As shown in Table I, electrical conductivity of acid formic is very high (884  $\mu\text{S}/\text{cm}$ ) while that of chloroform is very low (0.13  $\mu\text{S}/\text{cm}$ ). So, mixed solvent has a much lower conductivity (359  $\mu\text{S}/\text{cm}$ ) in comparison with acid formic. The conductivity of solvent affects the conductivity of solution severely. The electrical conductivity of solutions is determined by the solvent polarity. Generally, the dielectric constant of the solvent provides a rough measure of a

solvent polarity. Dielectric constant of acid formic and chloroform is 58 and 4.8, respectively. Solvents with a dielectric constant of less than 15 are generally considered to be nonpolar.<sup>31</sup>

Formic acid consists of an effectively infinite network of hydrogen-bonds, so it has a great deal of hydrogen-bonding with polymer. But, adding chloroform as nonpolar solvent causes a reduction in solvent-polymer hydrogen bonding while polymer-polymer bonding increases. So, the viscosity of polymer solution increases too. This phenomenon happens more strongly in higher concentrations because of more entanglement of molecular chains in solution.

#### Nanofibers morphology in spinning triangle

Figure 2 shows the typical SEM images of nanofiber in spinning triangle together with the distribution of nanofibers diameter. The average diameter of nanofibers is shown in Table III. Statistical tests show that nanofibers diameters increased significantly in presence of chloroform in both concentrations.

The average diameters of nanofibers were increased from 246 to 1080 nm in 18 wt % concentration by adding chloroform, while it increased from 117 to 199 nm in polymer concentration of 10 wt %, due to the reduction in charge density of solution.

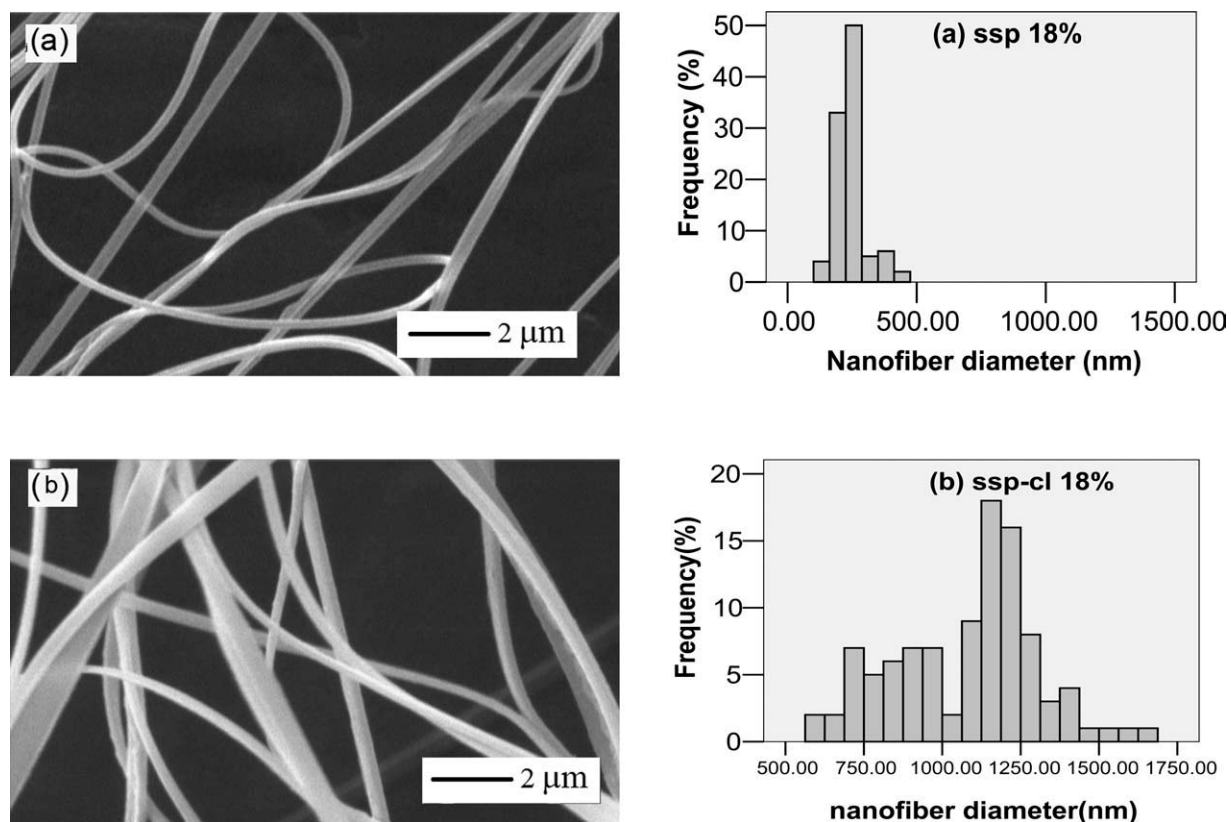


**Figure 2** SEM image of nanofiber in spinning triangle and diameter distribution: (a) SSP 18 wt % and (b) SSP-cl 18 wt %.



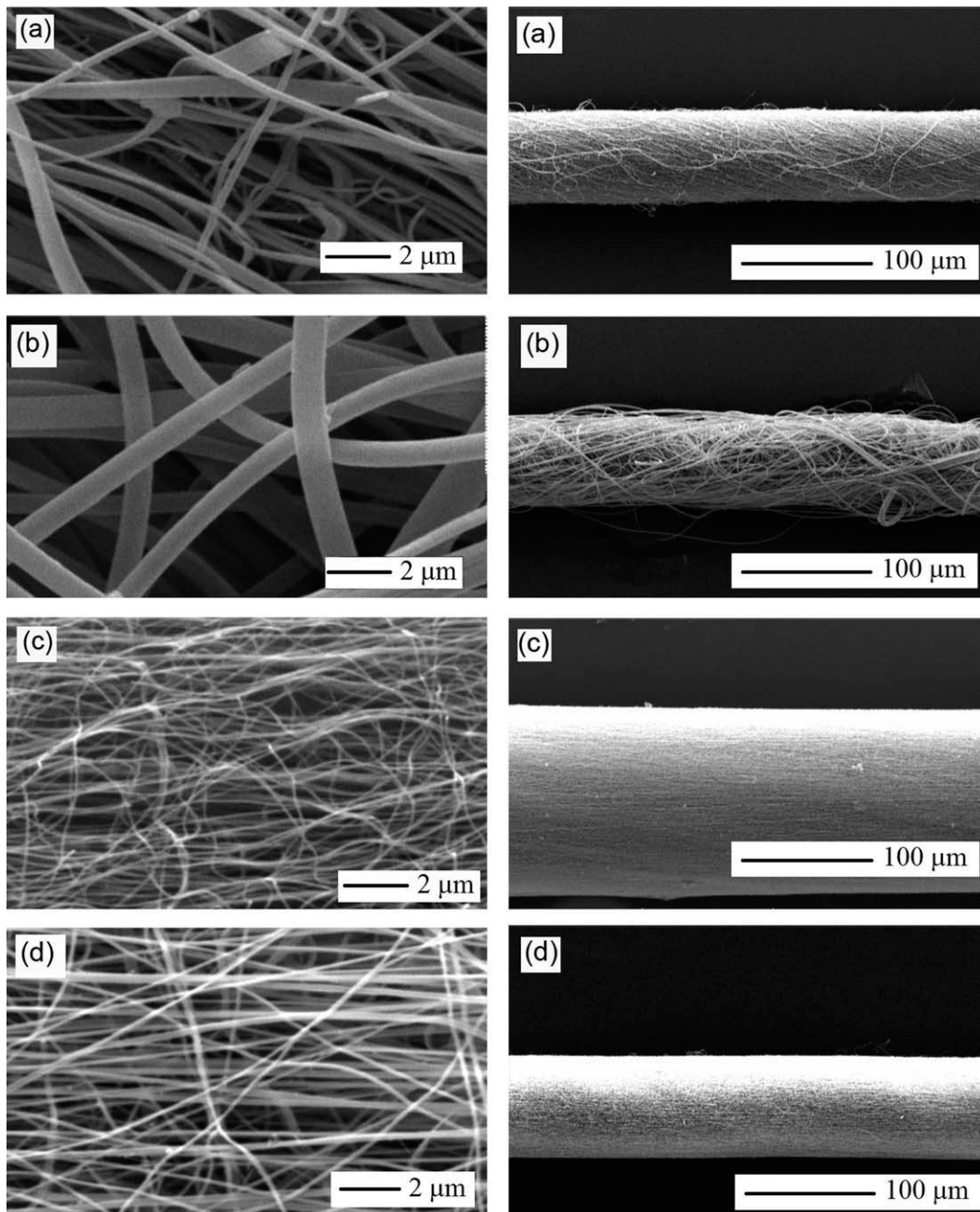


**Figure 3** SEM images of nanofibers yarn in two resolutions: (a) SSP 18 wt %, (b) SSP-cl 18 wt %, (c) SSP 10 wt %, and (d) SSP-cl 10 wt %.

As mentioned above, adding chloroform to formic acid causes a reduction in solvent polarity and electrical conductivity of solution. So, the higher dielectric constant of solvent causes the thinner nanofibers.<sup>32</sup> On the other hand, increasing zero-shear viscosity, due to adding chloroform, tends to increase the nanofibers diameter. These results corroborate similar observations in Refs. 33, 34.

#### Nanofibers yarn morphology

SEM images of produced nanofibers yarn of four solutions mentioned in Table III are shown in Figure 3.

As shown in Figure 3, nanofibers diameter of SSP-cl 10 and 18 wt % (b,d) obtained from mixed solvent has more uniformity than SSP 10 and 18 wt % (a,c) (see CV% of fiber diameter in Table III). The morphology of nanofibers obtained from mixed solvent (b,d) is a cylindrical rather than ribbon one; this observation indicates that adding chloroform is adequate for proper evaporation. But, the diameter of nanofibers electrospun from high concentration SSP-cl solution (18%) is too large (1080 nm) to form a uniform yarn. In this case, the effect of electrical forces in yarn production process decreased strongly and as a result, a nonuniform yarn was formed [Fig. 3(b)].

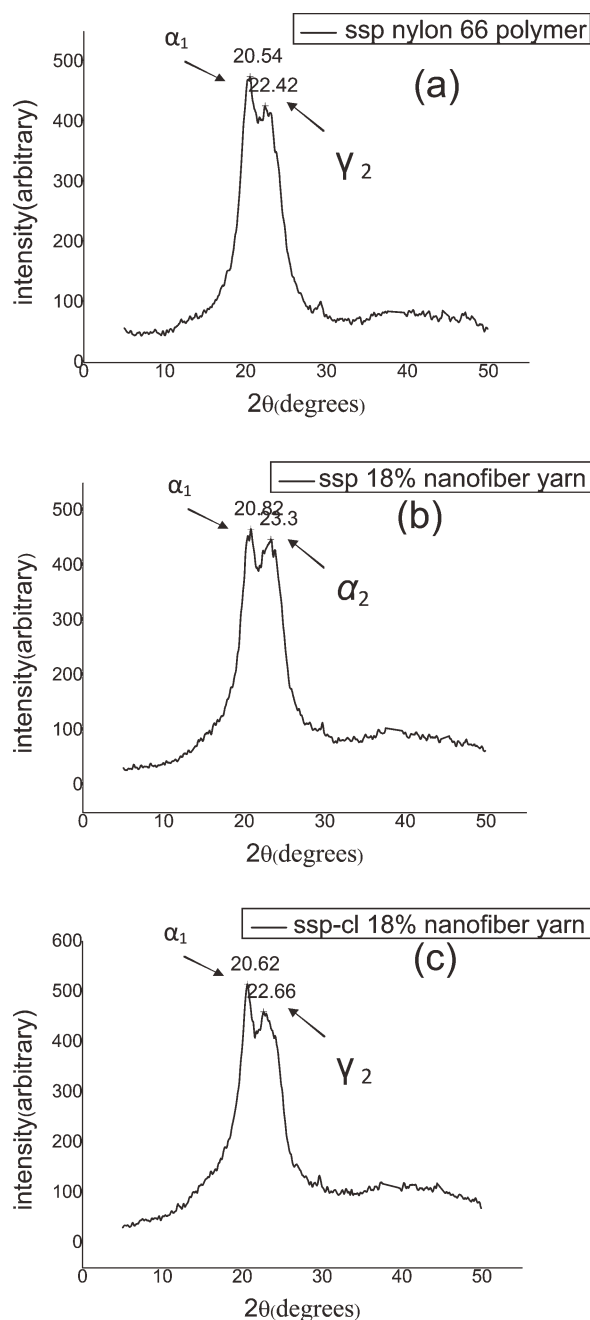


**Figure 4** XRD patterns of the (a) SSP PA66 polymer, (b) SSP 18% nanofiber yarn, and (c) SSP-cl 18% nanofiber yarn.

#### Crystallization behavior

XRD patterns were used to study the crystalline structure of both the neat PA66 polymer and the PA66 nanofiber yarns in two solvent types. Figure 4 shows XRD patterns acquired in reflectance mode for the neat polymer and the nanofiber yarns obtained in high concentration (18 wt %) of polymer solution.

XRD patterns show the characteristic of both  $\alpha$  as well as  $\gamma$  phases, the principal polymorphic structures found in polyamides.<sup>35</sup> The  $\alpha$  phase consists of

planar sheets of hydrogen-bonded chains with sheets stacked upon one another and displaced along the chain direction by a fixed amount. Pleated sheets of methylene units with hydrogen bonding between sheets rather than within sheets

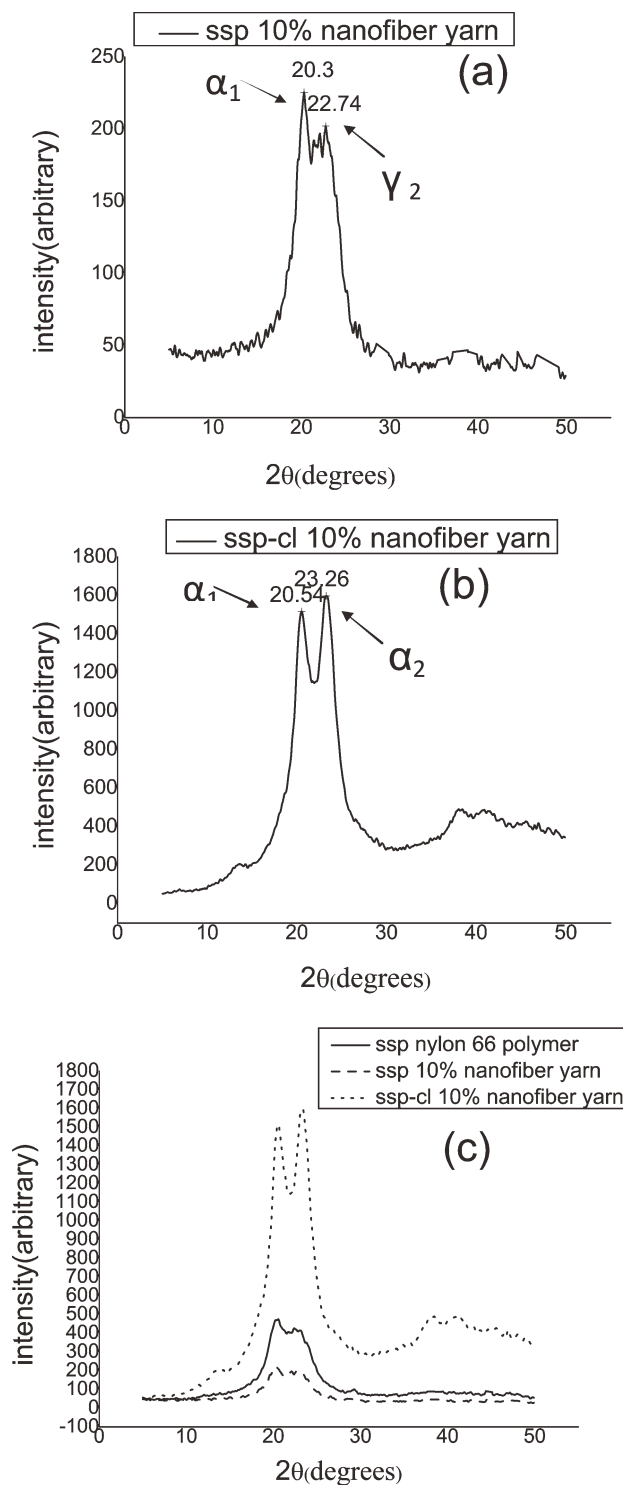


**Figure 5** XRD patterns of the (a) SSP 10% nanofiber yarn, (b) SSP-cl 10% nanofiber yarn, and (c) SSP PA66 polymer in comparison with the nanofiber yarns in two solvent systems.

**TABLE IV**  
Percent Crystallinity of the PA66 Nanofiber Yarns as Obtained from XRDs

Sample	Polymer	Nanofiber yarn			
	SSP PA66	SSP 18 wt %	SSP-cl 18 wt %	SSP 10 wt %	SSP-cl 10 wt %
Crystallinity (%)	30.7	30.4	25.6	28.5	43.1

characterize the  $\gamma$  phase. In SSP PA66 polymer, the two strong diffraction peaks at  $2\theta = 20.54^\circ$  and  $22.42^\circ$  are the distinctive feature of the  $\alpha$  and  $\gamma$  phase of PA66, which are designated as  $\alpha_1$  and  $\gamma_2$ . The  $\alpha_1$  peak arises from the distance between the hydrogen-bonded chains, and the  $\alpha_2$  peak arises from the separation of the hydrogen-bonded sheets.<sup>36</sup> The  $\gamma$  phase structure is unstable and seldom appears in PA66 at room temperature, as the  $\alpha$  phase is more stable than the  $\gamma$  phase. The existence of the  $\gamma$  phase at room temperature indicates the presence of additives added in the polymer to modify the properties. In SSP 18 wt % nanofibers yarn, the two strong diffraction peaks at  $2\theta = 20.82^\circ$  and  $23.3^\circ$  are  $\alpha_1$  and  $\alpha_2$ . XRD pattern of SSP-cl 18 wt % nanofibers yarn shows two strong diffraction peaks at  $2\theta = 20.62^\circ$  and  $22.66^\circ$  that are  $\alpha_1$  and  $\gamma_2$ . So, by adding chloroform, a reduction in  $\alpha_2$  peak means a reduction in hydrogen bonding between sheets and as a result, a decrease in crystallinity. It was observed that adding chloroform to produce nanofibers yarn influences the  $\alpha$  to  $\gamma$  crystal transformation in 18 wt % concentration.

Figure 5 shows the diffractograms of the neat polymer and the nanofiber yarns obtained in low concentration (10 wt %) of polymer solution.

In SSP 10 wt % nanofibers yarn [Fig. 5(a)], the two diffraction peaks at  $2\theta = 20.3^\circ$  and  $22.74^\circ$  are  $\alpha_1$  and  $\gamma_2$ . As shown in the XRD pattern of the SSP-cl 10 wt % nanofibers yarn [Fig. 5(b)], the two strong diffraction peaks at  $2\theta = 20.54^\circ$  and  $23.26^\circ$  are  $\alpha_1$  and  $\alpha_2$ . Contrary to the previous result, adding chloroform in the low concentration highly increases the degree of crystallinity of produced nanofibers yarn as shown in Figure 5(c). Table IV shows the percent crystallinity of the nanofiber yarns as obtained from

XRD patterns. The results reveal that adding chloroform in high concentration solution tends to decrease percent crystallinity of nanofibers yarn, whereas in the low concentration the crystallinity increases.

#### Mechanical properties of nanofiber yarns

Table V shows the mechanical properties of electrospun PA66 yarns in 10 and 18 wt % concentrations that were made with two solvent types. It is evident that the solvent type influenced morphology and crystallinity of the produced nanofibers as mentioned above; therefore, it affected the elongation at break, initial modulus and the strength of yarns.

In the 18 wt % solution, adding chloroform decreased the initial modulus as well as the strength of nanofiber yarns, whereas in 10 wt %, adding chloroform increased these properties according to the crystallinity percent of the nanofiber yarns.

Surface tension of the low concentration polymer solution overcomes the viscosity and the electrical forces in the electrospinning process. According to Table I, adding chloroform decreased the surface tension of the polymer solution. So, the effect of electrical forces increased and the polymer solution stretched more and more and the final nanofiber orientation increased.

It is well known that most electrospun filaments are not oriented and therefore, exhibit poor mechanical properties, namely, the initial modulus and the strength.<sup>12</sup> Interestingly, this study clearly shows that the modulus and the strength are much higher for the nanofiber yarns made from the PA66 in low concentration with chloroform than in high concentration (see Table V).

**TABLE V**  
Mechanical Properties of Electrospun SSP PA66 Yarns in Two Solvent Systems

Sample	Number of tests	Mean linear density		Tenacity		Extension at $F_{max}$		E-modulus		
		den	CV %	MPa	CV %	%	CV %	MPa	CV %	
1	SSP 18 wt %	30	27.77	13.48	88.01	31.35	43.71	34.04	967.86	32.51
	SSP-cl 18 wt %	30	31.72	45.52	45.03	27.85	34.01	48.16	657.89	34.21
2	SSP 10 wt %	30	13.53	17.66	90.86	13.68	42.37	21.88	544.81	21.26
	SSP-cl 10 wt %	30	17.21	21.93	120.16	16.32	46.79	16.95	1216.27	24.97

**TABLE VI**  
Zero Shear Viscosity,  $\eta_0$ , and the Nanofiber Diameter with Increase in Concentration

Sample	Solution concentration, C (wt %)	Zero shear viscosity, $\eta_0$ (cP)	Fiber diameter	
			Number-average (nm)	CV %
1	SSP 10 %	324	117	16.03
2	SSP 14 %	1615	196	28.83
3	SSP 18 %	2479	246	25.9

**TABLE VII**  
Effect of Solution Concentration on the Mechanical Properties of Electrospun PA66 Yarns

Sample	Number of tests	Mean linear density		Tenacity		Extension at $F_{max}$		E-modulus	
		den	CV %	MPa	CV %	%	CV %	MPa	CV %
SSP 10 wt %	30	13.53	17.66	90.85	13.68	42.37	21.88	544.81	21.26
SSP 14 wt %	30	29.38	23.7	93.14	23.26	56.32	14.29	573.88	34.78
SSP 18 wt %	30	27.77	13.48	88	31.35	43.71	34.04	1228.5	71.28

### Solution concentration

The results presented in Table VI illustrate the effect of polymer solution concentration on the nanofibers diameter. The results reveal that nanofibers diameter and viscosity of polymer solution tend to increase with increasing polymer solution concentration.

Table VII shows the effect of solution concentration on mechanical properties of nanofiber yarns. The modulus of nanofiber yarns increased in higher concentrations but, the strength has no significance difference.

### CONCLUSIONS

SSP PA66 nanofiber yarns were electrospun with two oppositely metallic spinnerets system in different conditions. XRD patterns suggested the presence of chloroform in the PA66/formic acid solution with the concentration of 18 wt % influencing the transformation of PA66 nanofiber yarn from  $\alpha$  phase crystals to a mixture of  $\alpha$  and  $\gamma$  phase crystals; it means a decrease in crystallinity. At the same time, adding chloroform in the PA66/formic acid solution with the concentration of 10 wt % facilitated the mixture of  $\alpha$  and  $\gamma$  phase crystals to  $\alpha$  crystal transformation. In this case, crystallinity tends to increase from 28.5 to 43.1%. This study clearly shows that the modulus and the strength are much higher for the nanofiber yarns made from the PA66 of 10 wt % solution in the presence of chloroform and for that of 18 wt % solution. Thus, the combination of formic acid and chloroform as a solvent in low concentration polymer solution results in enhancements in the structural and mechanical properties of PA66 nanofiber yarn. The increase in solution concentration makes

no significant difference in the strength of nanofiber yarns, while the modulus of the nanofibers yarn increases significantly.

### References

- Li, D.; Xia, Y. N. *Adv Mater* 2004, 16, 1151.
- Yarin, A. L.; Koombhongse, S.; Reneker, D. H. *J Appl Phys* 2001, 89, 3018.
- Wang, X. Y.; Drew, C.; Lee, S. H.; Senecal, K. J.; Kumar, J.; Samuelson, L. A. *J Macromol Sci Pure Appl Chem* 2002, 39, 1251.
- Kim, J.; Jia, H. F.; Wang, P. *Biotechnol Adv* 2006, 24, 296.
- Ramakrishna, S.; Fujihara, K.; Teo, W. E.; Yong, T.; Ma, Z. W.; Ramaseshan, R. *Mater Today* 2006, 9, 40.
- Qin, X. H.; Wang, S. Y. *J Appl Polym Sci* 2006, 102, 1285.
- Murugan, R.; Ramakrishna, S. *Tissue Eng* 2006, 12, 435.
- Jose, M. V.; Steinert, B. W.; Thomas, V.; Dean, D. R.; Abdalla, M. A.; Price, G.; Janowski, G.M. *Polymer* 2007, 48, 1096.
- Zheng, J.; He, A.; Li, J.; Xu, J.; Han, C. C. *Polymer* 2006, 47, 7095.
- Li, D.; Wang, Y.; Xia, U. *Nano Lett* 2003, 3, 1167.
- Pan, H.; Li, L.; Hu, L.; Cui, X. *Polymer* 2006, 47, 4901.
- Teo, W. E.; Ramakrishna, S. *Nanotechnology* 2006, 17, 89.
- Sarkar, S.; Deevi, S.; Tepper, G. *Macromol Rapid Commun* 2007, 28, 1034.
- Fang-Lei, Z.; Rong Hua, G. *Polym Int* 2008, 57, 622.
- Pan, H.; Li, L.; Hu, L.; Cui, X. *Polymer* 2006, 47, 4901.
- Dabirian, F.; Hosseini, Y.; Hosseini Ravandi, A. *J Tex Ins* 2007, 98, 237.
- Khil, M. S.; Bhattarai, S. R.; Kim, H. Y.; Kim, S. Z.; Lee, K. H. *J Biomed Mater Res* 2005, 72, 117.
- Smith, E.; Buttner, U.; Sanderson, R. D. *Polym Commun* 2005, 46, 2419.
- Teo, W. E.; Gopal, R.; Ramaseshan, R.; Fujihara, K.; Ramakrishna, S. *Polymer* 2007, 48, 3400.
- Dabirian, F.; Hosseini, S. A. *Fibres Text Eastern Eur* 2009, 17, 45.
- Doshi, J.; Reneker, D. H. *J Electrostatics* 1995, 35, 151.
- Zong, X.; Kim, K.; Fang, D.; Ran, S.; Hsiao, B. S.; Chu, B. *Polymer* 2002, 43, 4403.



23. Martin, G. E.; Cockshott, I. D.; Fildes, F. J. T. US Patent 4,044,404 (1975).
24. Tsai, P. P.; Chen, W. *Int Nonwovens J* 2004, 13, 17.
25. Jung, D. *Fiber and Polymer Science*, A dissertation submitted to the Graduate Faculty of North Carolina State University, 2004.
26. Zussman, E.; Burman, M.; Yarin, A. L.; Khalfin, R.; Cohen, Y. *J Polym Sci: B: Polym Phys* 2006, 44, 1482.
27. Huber, A.; Pickett, A.; Shakesheff, K. M. *Eur Cells Mater* 2007, 14, 56.
28. Lingaiah, S.; Shivakumar, K. N.; Sadler, R. L. 49th American Institute of Aeronautics and Astronautics, Structures, Structural Dynamics, and Materials Conference, 7–10 April 2008, Schaumburg, IL.
29. Guerrini, L. M.; Branciforti, M. C.; Canova, T.; Bretas, R. E. S. *Materials Research* 2009, 12, 181.
30. Gogolewski, S.; Pennings, A. J. *Polymer* 1985, 26, 1394.
31. Lowry, T. H.; Richardson, K. S. *Mechanism and Theory in Organic Chemistry*, 3rd ed. Benjamin-Cummings Publishing Company, 1987.
32. Won, K. S.; Youk, J. H.; Taek, S. L.; Won, H. P. *Polymer* 2004, 45, 2959.
33. Fong, H.; Chun, I.; Reneker, D. H. *Polymer* 1999, 40, 4585.
34. Deitzel, J. M.; Kleinmeyer, J. D.; Harris, D.; Beck, Tan, N. C. *Polymer* 2001, 42, 261.
35. Ho, J.; Wei, K. *Macromolecules* 2000, 33, 5181.
36. Vasanthan, N.; Murthy, N. S.; Bray, R. G. *Macromolecules* 1998, 31, 8433.